Environment International 130 (2019) 104852

Contents lists available at ScienceDirect

Environment International

journal homepage: www.elsevier.com/locate/envint

Enzymatic hydrolysis of poly(1,4-butylene 2,5-thiophenedicarboxylate) (PBTF) and poly(1,4-butylene 2,5-furandicarboxylate) (PBF) films: A comparison of mechanisms

Matteo Gigli[a,1], Felice Quartinello[b,1], Michelina Soccio[c], Alessandro Pellis[b,d,*], Nadia Lotti[c,**], Georg M. Guebitz[b,e], Silvia Licoccia[a], Andrea Munari[c]

[a] University of Roma Tor Vergata, Department of Chemical Science and Technologies, Via della Ricerca Scientifica 1, 00133 Roma, Italy
[b] University of Natural Resources and Life Sciences, Vienna, Department of Agrobiotechnology, Institute of Environmental Biotechnology, Konrad Lorenz Strasse 20, 3430 Tulln an der Donau, Austria
[c] University of Bologna, Department of Civil, Chemical, Environmental and Materials Engineering, Via Terracini 28, 40131 Bologna, Italy
[d] University of York, Department of Chemistry, Green Chemistry Centre of Excellence, YO10 5DD Heslington, York, UK
[e] Austrian Centre of Industrial Biotechnology, Konrad Lorenz Strasse 20, 3430 Tulln an der Donau, Austria

ARTICLE INFO

Handling Editor: Thanh Nguyen

Keywords:
Poly(1,4-butylene 2,5-thiophenedicarboxylate) (PBTF)
Poly(1,4-butylene 2,5-furandicarboxylate) (PBF)
Enzymatic hydrolysis
Endo/exo chain scission
Cutinases
Polyesters degradation

ABSTRACT

Enzymatic hydrolysis of poly(1,4-butylene 2,5-thiophenedicarboxylate) (PBTF) and poly(1,4-butylene 2,5-furandicarboxylate) (PBF) by *Humicola insolens* (HiC) and *Thermobifida cellulosilytica* (Cut) cutinases is investigated. For the first time, the different depolymerization mechanisms of PBTF (*endo*-wise scission) and PBF (*exo*-wise cleavage) has been unveiled and correlated to the chemical structure of the two polyesters.

1. Introduction

The constantly emerging problems deriving from plastic pollution such as the accumulation of manmade materials in the great pacific garbage patch and the increasing amounts of polymers accumulated by wildlife are a current threat to our planet Earth that needs to be tackled by mankind in a timely manner (Lebreton et al., 2018; Foekema et al., 2013).

Efforts in this direction have already been made especially from Europe that plans a ban of certain products (plastic cotton buds, cutlery, etc.) and a consumption reduction for other goods (plastic food containers and drinks cups). Moreover, obligations for producers will be introduced, with industries that will also be given incentives to develop ecofriendly alternatives for these products (https://ec.europa.eu/commission/news/single-use-plastics-2018-may-28_en, n.d.). Giant leaps forward on industrial scale production of more benign plastics have already been made, especially for the substitution of the petrol-based poly(ethylene terephthalate) (PET), the main component of water and soft drink bottles. Nowadays in fact, the diol component (ethylene glycol) of PET materials is already derived from renewable resources, but accounts only for 20–30% of the total weight of the material. (https://www.coca-cola.co.uk/faq/what-is-plantbottle, n.d.) Researchers around the world are now trying to derive the diacid component, terephthalic acid (TA), from renewable resources, (Pellis et al., 2016a) or focus on the development of biobased TA-free polyesters. In this framework, the most well-known example is 2,5-furandicarboxylic acid (FDCA), already obtainable from biomass at large scale (Kim et al., 2018; de Jong et al., 2012). Starting from FDCA, a PET substitute named poly(ethylene 2,5-furanoate) (PEF) has been produced, together with a series of FDCA-based polyesters containing diols with various carbon chain lengths (usually between 2 and 12 C atoms) (Papageorgiou et al., 2016; Pérocheau Arnaud et al., 2017; Wang et al., 2017; Papageorgiou et al., 2014) and some lignin-derived pyridine-based polyesters (Pellis et al., 2019). Together with a bio-based character and outstanding gas barrier behavior, FDCA-based polymers turned out to be also more biodegradable than their TA-based

* Correspondence to: A. Pellis, University of York, Department of Chemistry, Green Chemistry Centre of Excellence, YO10 5DD Heslington, York, UK.
** Corresponding author.
E-mail addresses: alessandro.pellis@gmail.com (A. Pellis), nadia.lotti@unibo.it (N. Lotti).
[1] Dr. Matteo Gigli and Mr. Felice Quartinello equally contributed to the work.

https://doi.org/10.1016/j.envint.2019.05.046
Received 19 March 2019; Received in revised form 29 April 2019; Accepted 16 May 2019

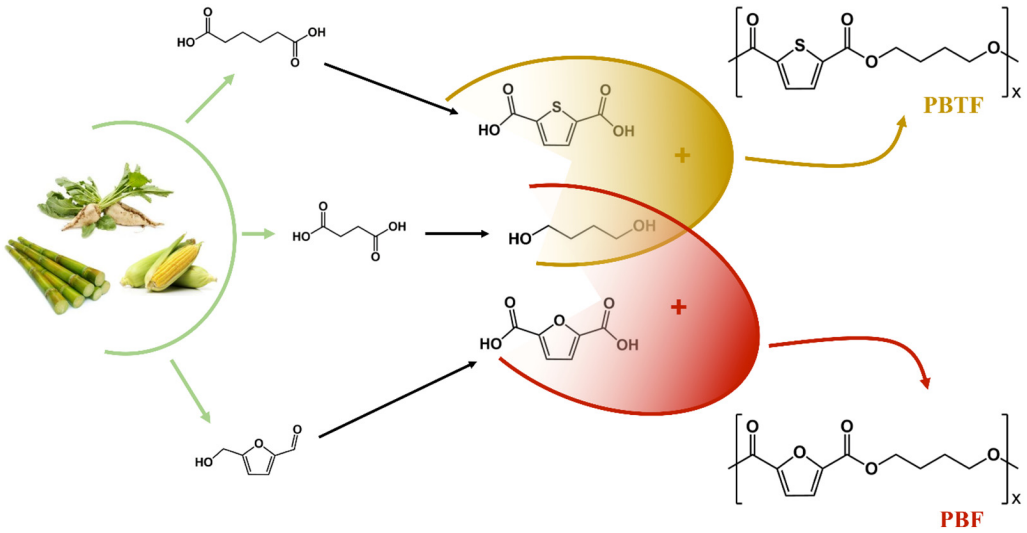

Scheme 1. Synthesis of PBF and PBTF and highlight on the monomer's precursors derived from renewable resources.

counterparts using enzymes as biocatalyst. In fact, while the degradation of PET requires several days, and in most cases does not reach completion, (Wei et al., 2016; Then et al., 2016; Gamerith et al., 2017) the hydrolysis of PEF thin films was reported to be complete in 72 h when using the cutinase from *Humicola insolens* in well-controlled in vitro conditions (Pellis et al., 2016b; Weinberger et al., 2017b).

More recently, the use of 2,5-thiophenedicarboxylic acid (TFDCA) as alternative for the synthesis of high-performance polyesters and of various monomers for the synthesis of PET-like materials were also suggested (Guidotti et al., 2018a; Guidotti et al., 2018b). In particular, PBTF revealed smart mechanical and barrier properties, these last comparable to those of furanoate-based polyesters (Guidotti et al., 2018c; Guidotti et al., 2018d). In the present work, the enzymatic degradability of PBTF is demonstrated for the first time and compared to that of PBF. In addition, the hydrolysis mechanism associated to the used biocatalysts was elucidated (Scheme 1).

2. Results and discussion

The PBTF and PBF powders displayed a similar molecular weight (M_n = 37,300, PDI = 1.6 and M_n = 33,900, PDI = 1.7, respectively). Both polymers show a high melting temperature and a comparable associated melting enthalpy: T_m = 149 °C and ΔHm = 28 J/g (PBTF) and Tm = 160 °C and ΔHm = 25 J/g (PBF). On the other hand, PBTF chains (T_g = 25 °C) are more mobile than PBF (T_g = 39 °C) ones, because of the lower glass transition temperature, in turn caused by the weaker interchain interactions, as previously observed (Guidotti et al., 2018d).

Following recent works that demonstrated the efficient degradation of amorphous PEF using cutinases, (Weinberger et al., 2017a; Weinberger et al., 2017b) in this study we compared the hydrolysis of PBTF and PBF by two different enzymes, a commercial cutinase from *Humicola insolens* (HiC) and the thermostable *Thermobifida cellulosilytica* cutinase 1 (Cut).

The polymeric thin films were appropriately cut and cleaned from contaminants as described in the M&M section. Enzymatic hydrolyses were carried out for 72 h using a 5 μM enzyme concentration in 1 M K_2HPO_4/KH_2PO_4 buffer at pH 8, conditions that were reported to be the best for the hydrolysis of PEF thin films (Weinberger et al., 2017a). Weight loss results are shown in Fig. 1 and indicate that both enzymes are fairly active in the hydrolysis of the two polymers. More in detail, while for PBTF the weight loss is rather similar (18%) for both enzymes at both selected operational temperatures, in the case of PBF both enzymes are more active at 65 than 50 °C, as demonstrated by the higher weight loss after 72 h of reaction (12 vs 15% for Cut and 16 vs 24% for HiC). To better understand the enzymatic hydrolysis of the two polymers, HPLC analysis of the released molecules was performed.

Fig. 2 shows that while for PBF the increase of FDCA concentration nicely corresponds to the weight loss (Fig. 1), the released TFDCA follows a completely different trend when compared to the weight loss data. After a low amount of soluble TFDCA detected after 24 (0.44 and 0.74 mM for Cut and HiC respectively at 65 °C) and 48 h (0.84 and 1.29 mM for Cut and HiC respectively at 65 °C), the amount of the sulfur-containing aromatic diacid increases to 1.20 and 3.40 mM for Cut and HiC respectively at 65 °C.

To highlight the effect of enzymatic hydrolysis on PBTF and PBF films, ATR-FTIR spectra have been recorded on partially hydrolyzed specimens (Fig. 3). Samples incubated at 65 °C and 72 h have been considered, being these conditions the most effective for enzymatic attack. Pristine samples have been also analysed for sake of comparison. In particular, the following peaks of the absorbance spectrum are of interest: 1) the peak located at 1701 (PBTF) - 1709 (PBF) cm^{-1}, which can be assigned to the C=O stretching, 2) the peak located at 1234 (PBTF) - 1267 (PBF) cm^{-1} attributed to the C-O-C stretching from an ester group and 3) the peak situated at 742 (PBTF) - 764 (PBF) cm^{-1} from the ring bending vibration (Xie et al., 2019; Araujo et al., 2018).

It can be noted that the peak at 1700 cm^{-1} does not undergo any changes when comparing pristine PBF films with degraded ones. On the other hand, in the case of PBTF, an enlargement of the peak in the region just below 1700 cm^{-1}, relative to the C=O stretching from carboxylic groups, (Terzopoulou et al., 2017) can be observed. The effect is more intense in the case of HiC-hydrolyzed films. Furthermore, the ratio between the peak at 750 cm^{-1} ca. and that at 1250 cm^{-1} ca., which represents the ratio between furan (or thiophene) rings and ester groups, remains practically unaltered in PBF (Fig. 3B), while for PBTF a significant change, due to the lowering of the intensity of the peak at 1234 cm^{-1}, is visible (Fig. 3A).

In particular, the ratio between the above mentioned peaks is equal to 0.93 for pristine PBF, 0.90 for Cut-hydrolyzed and 0.94 for HiC-hydrolyzed films. On the other hand, for PBTF, a ratio equal to 0.90, 0.98 and 1.11 for pristine, Cut- and HiC-hydrolyzed samples has been calculated, respectively, meaning that the concentration of ester groups as compared to the amount of thiophene rings is decreased. As measured, the effect is more evident for PBTF films incubated in the presence of HiC.

Altogether, the observed results suggest a different hydrolysis mechanism of the two polymers: PBTF seems to be mostly hydrolyzed via an *endo*-wise mechanism, while PBF appears to be preferentially

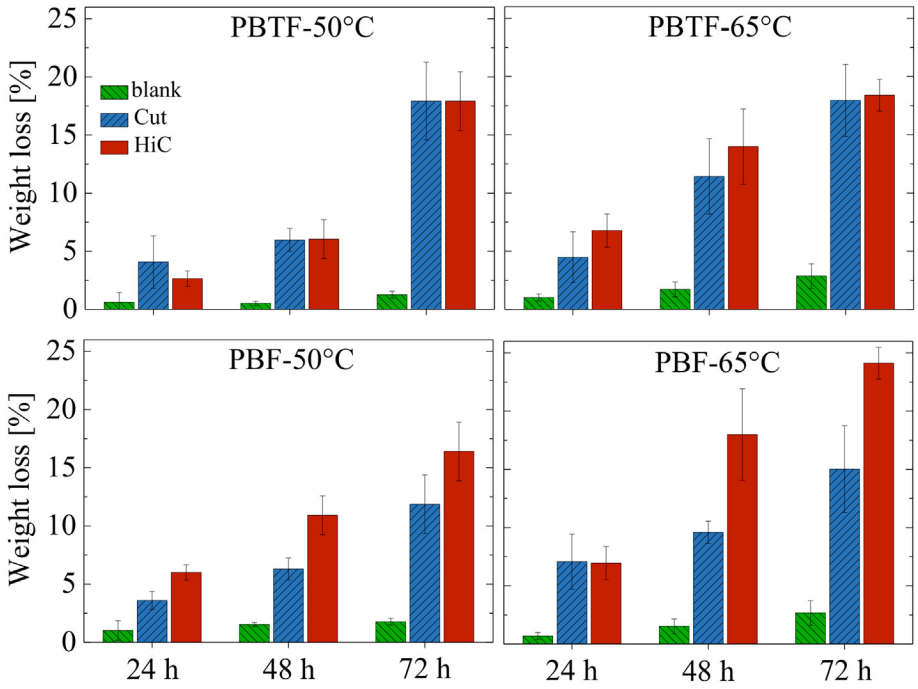

Fig. 1. Weight loss of PBF and PBTF after enzymatic hydrolysis at 50 and 65 °C. All experiments were performed in triplicates and are shown ± the standard deviation.

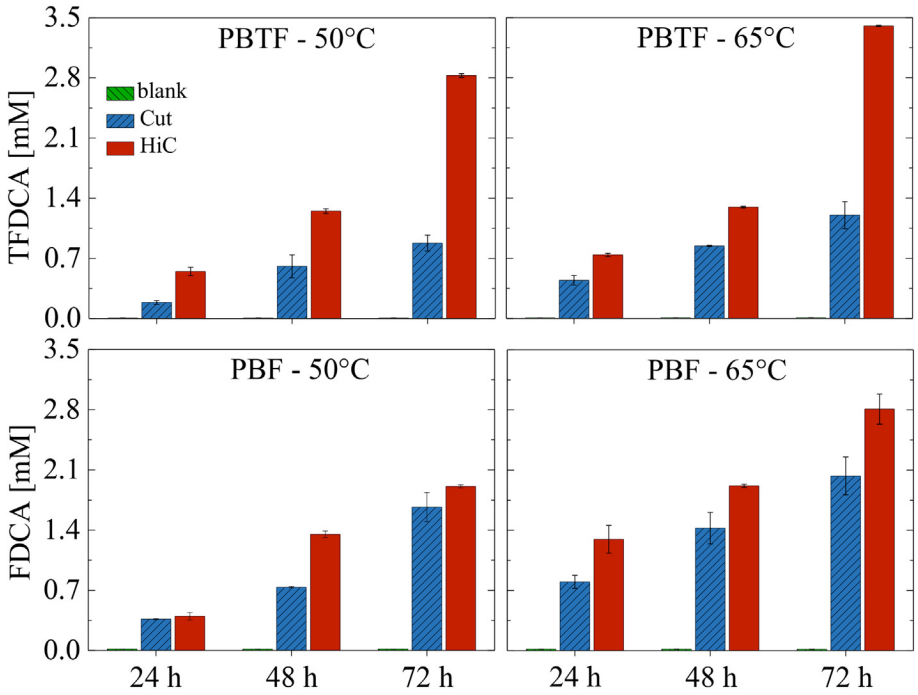

Fig. 2. Solubilized molecules during enzymatic hydrolysis of PBF and PBTF. All experiments were performed in triplicates and are shown ± the standard deviation.

cleaved *exo*-wise.

In fact, in an endo-wise attack, ester bonds are randomly cleaved along the polymer backbone, thus initially leading to insoluble oligomers. Successively, when shorter soluble oligomers are formed, they can easily be broken down to monomers by the enzyme action. This would explain both the increase in the ester to acid group concentration and the enhancement of the ring to ester group concentration, evidenced by the ATR-FTIR studies of PBTF films (Fig. 3A) and the spike in TFDCA concentration after 72 h of incubation (Fig. 2). Conversely, in an *exo*-wise mechanism a linear increase of monomer concentration can be observed (Fig. 2), as due to the cleavage of terminal units of the polymer chains. In this case, the ratio between ester and acid groups and between ester groups and furan rings should not vary, as observed by ATR-FTIR measurements (Fig. 3B). Lastly, it can be noticed that HiC shows a higher activity with respect to Cut. A schematic representation of the endo/exo cutting of the polymer chains by the enzymes is shown in Fig. 4.

The two distinct hydrolysis mechanisms can be explained on the basis of the different properties of thiophene and furan rings. Indeed, although the two polymers display a similar chemical structure, both

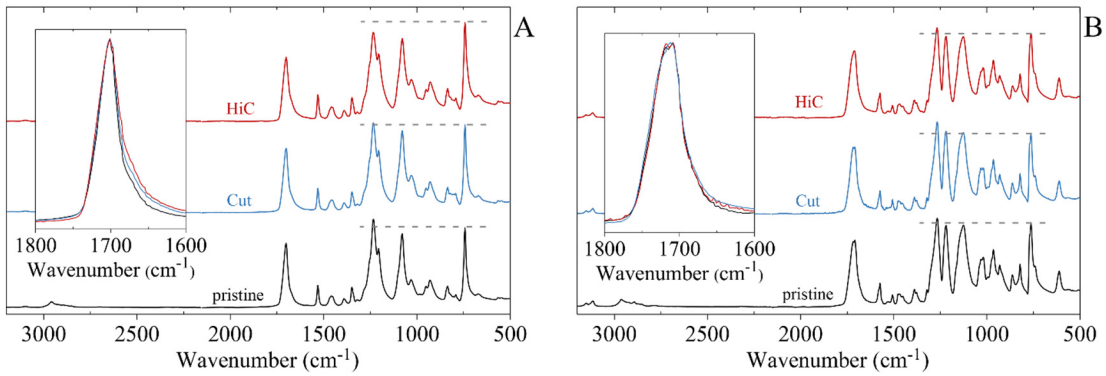

Fig. 3. ATR-FTIR spectra of partially hydrolyzed PBTF (A) and PBF (B) films. In the inset, the region around 1700 cm^{-1} has been highlighted. All spectra have been normalized with respect to the intensity of the peak located at 1700 cm^{-1}. Dashed lines represent guides for the eyes.

containing heteroaromatic five-membered rings connected by the same glycol subunit, the properties of the two polymers are quite diverse. More in detail, the higher electronegativity of the oxygen as compared to the sulfur atom causes not only a lower aromaticity of the furan ring, but also a higher ring dipole moment, resulting in stronger interchain interactions, due to hydrogen bonding between the protons on the ring and the carbonyl of an adjacent polymer chain. (Guidotti et al., 2018b; Araujo et al., 2018).

As a consequence, PBF chains are less mobile (T_g = 39 °C for PBF vs 25 °C for PBTF) and less accessible to the cutinases with respect to PBTF ones, thus the random scission of ester bonds along the polymer chains is impeded.

The results here described well fit and explain those already reported in the literature. Indeed, it has been reported the PEF hydrolysis by the same cutinases adopted in the present work (Gamerith et al., 2017) and the *endo*-wise ester cleavage of poly(ethylene terephthalate) PET (Eberl et al., 2009). In their work, Eberl and co-workers compared the action of a cutinase enzyme really similar to the Cut here employed (cutinase from *Thermobifida fusca*) with a lipase from *Thermomyces lanuginosus* and a cutinase from *Fusarium solani* for the hydrolysis of PET fabrics and films and some related model compounds. The report concludes that all tested hydrolase enzymes are able to hydrolyze PET via an endo-wise mechanism. Albeit not stated in the work, it can be hypothesized that the absence of hydrogen bonding allows indeed for the random cleavage of esters along the PET backbone by the used enzymes. SEM analyses nicely support the above discussed results. The proceeding of the hydrolysis is well evidenced in Fig. 5: by increasing the incubation time, the film surface, initially smooth and defect-free, appears more and more notched by the enzyme action. The different hydrolysis mechanisms of HiC on the two polymers can be noticed, too. Preferential areas of hydrolysis are visible on the PBTF surface, where much bigger and isolated craters (above 10 μm of diameter) can be clearly spotted, while PBF seems uniformly and randomly degraded as due to the small holes distributed on the entire film surface.

Also, the enhanced enzymatic activity at 65 °C and the more effective attack of HiC with respect to Cut is highlighted in Fig. 6, which contains SEM micrographs of PBTF and PBF films after 48 h of incubation.

Indeed, the diverse HiC action on the two polymers is confirmed also at higher temperatures, though a higher degradation extent can be observed. On the other hand, by comparing the partially degraded film surfaces appear evident how both polymers are less affected by Cut action as compared to HiC. Additional MALDI analysis does not reveal significant differences between pristine and hydrolyzed samples. This is somehow expected, taking into account that the enzymatic hydrolysis is a surface eroding process, and MALDI a bulk technique, capable of detecting only major changes in the polymer's molecular weight, as previously demonstrated for the *Humicola insolens* cutinase-catalyzed surface hydrolysis of poly(lactic acid) thin films (Pellis et al., 2015).

3. Experimental

3.1. Materials

TFDCA (97%) was purchased from TCI (Tokyo, Japan). Hexafluoro-2-propanol, chloroform, methanol, 1,4-butanediol (BD, 99%), titanium tetrabutoxide (TBT, 97%) and titanium isopropoxide (TTIP, 97%) were obtained from Sigma Aldrich (Saint Louis, MO, USA). TBT and TTIP were distilled before use, while all other products have been used as received.

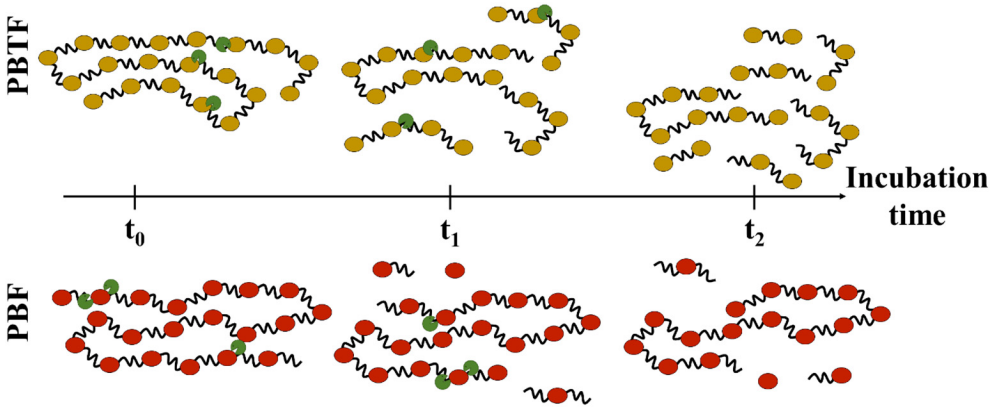

Fig. 4. Enzymatic hydrolysis mechanisms. The *endo*-wise hydrolysis mechanism for PBTF (top) leads to the release of oligomers, which are subsequently hydrolyzed to monomers. In contrast, the *exo*-wise hydrolysis mechanism for PBF (bottom) leads to the immediate release of monomers.

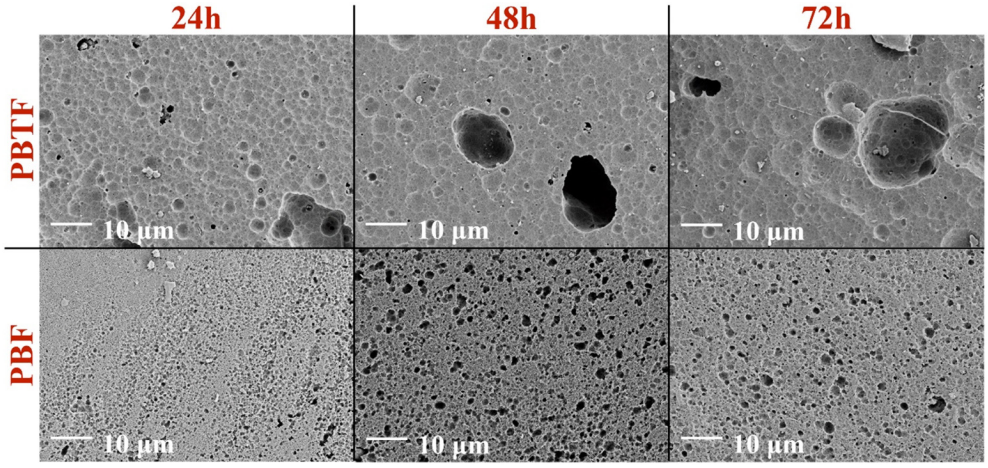

Fig. 5. SEM micrographs (5000 X) of partially degraded PBTF and PBF films incubated at 50 °C in the presence of 5 µM HiC.

3.2. Polymer synthesis, characterization and film preparation

PBTF and PBF were synthesized through two-step melt polycondensation by respectively reacting TFDCA and FDCA with 4-folds molar excess of BD and using 150 ppm/$g_{polymer}$ of TBT and 150 ppm/$g_{polymer}$ of TTIP as catalysts, in accordance to the procedure previously described with minor modifications (Guidotti et al., 2018d; Soccio et al., 2016).

Briefly, the reaction mixture was heated to 170–180 °C in a silicon oil bath under nitrogen flow and stirred at 100 rpm by a two-bladed centrifugal stirrer connected to an overhead motor (IKA-Werke GmbH & Co., Staufen, Germany). When more than 90% of the water produced during esterification was distilled off, pressure and temperature were gradually decreased to 0.1 mbar and increased to 200–210 °C, respectively. Polymerization was stopped when constant torque was measured. Films in the range 100–200 µm were obtained by compression molding (Specac Atlas manual hydraulic press, Orpington, UK). Polymer powder was placed in between two teflon plates and heated to 180 °C (PBTF) or 190 °C (PBF). A pressure of 5 tons m^{-2} was applied for 2 min. Films were cooled to 20 °C in the press thanks to a home-made refrigeration system that uses tap water. Molecular weight was determined by gel permeation chromatography (GPC) at 30 °C on a Agilent 1100 HPLC system (Santa Clara, CA, USA) equipped with PLgel 5-µm MiniMIX-C column. Hexafluoro-2-propanol/chloroform mixture (5:95 *v*/v) was used as eluent (0.3 mL min^{-1}). Polystyrene standards in the range 800–100,000 g/mol were used for the calibration. Thermal transitions were recorded on A Perkin Elmer DSC6 (Waltham, MA, USA) by heating the samples from −20 to 200 °C at 20 °C min^{-1}.

ATR-FTIR spectra were recorded on a FT-IR Nicolet IS5 (Thermo Fisher Scientific, Whaltman, MA, USA) over the 500–3300 cm^{-1} range using 32 scans in absorbance mode.

3.3. Protein quantification and esterase activity assay

Protein concentration was measured using the Bio-RadProtein Assay Kit (Bio-Rad, Vienna, Austria). Bovine Serum Albumin (BSA) was used as protein standard; 10 µL of the sample were added into the wells of a 96-well plate. Afterwards, 200 µL of the prepared Bio-Rad reagent solution was added (Bio-Rad Reagent diluted 1:5 with ultrapure water). The plate was incubated for 5 min at 21 °C and 400 rpm. Buffer (1 M potassium phosphate pH 8) was used as blank. The absorption after 5 min was measured at λ = 595 nm in a plate reader (Tecan INFINITE M200) and the concentration calculated from the average of triplicates.

Esterase activity was measured at 25 °C using *p*-nitrophenyl-butyrate (p-NPB) as a substrate according to Pellis et al. (Pellis et al., 2015). The final assay was carried out by mixing 200 µL of the substrate stock solution, 1 M potassium phosphate pH 8, with 20 µL of enzyme solution. The increase in the absorbance at 405 nm due to the release of p-nitrophenol (ε 405 nm = 10.27 mL (µmol cm)$^{-1}$) was measured for 5 min, every 18 s with a plate reader. A blank was included using 20 µL of buffer instead of enzyme solution. The activity was calculated in units (U), where 1 unit is defined as the amount of enzyme required to hydrolyze 1 µmol of substrate per minute under the given assay conditions.

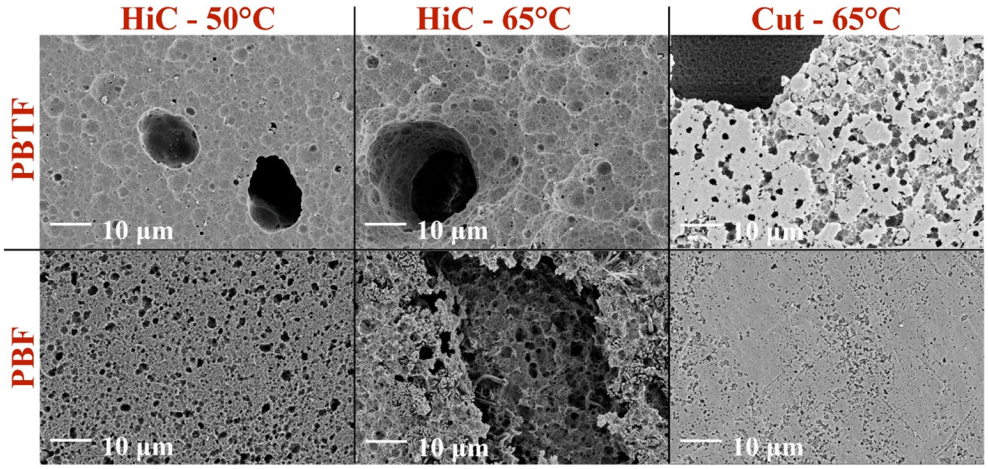

Fig. 6. SEM micrographs (5000 X) of PBTF and PBF films after 48 h of incubation with the indicated enzymes.

3.4. Enzymatic hydrolysis of PBF and PBTF thin films

PBF and PBTF were cut into 1 cm × 0.5 cm pieces. Three washing steps were performed to remove possible impurities from polymer surfaces. Then, the polymers were incubated with Triton X-100 (5 g L^{-1}), Na_2CO_3 (100 mM) and ultrapure water at 50 °C and 130 rpm. Afterward, each sample was dried overnight under a fume cupboard at 21 °C. The films were then incubated with 2 mL of 1 M potassium phosphate buffer pH 8, with *Humicola insolens* cutinase (HiC) or *Thermobifida cellulosilytica* cutinase 1 (Cut) with the final concentration of 5 μM. Incubations were performed at 50 and 65 °C, analogously with previous reports on PET and PEF hydrolysis (Gamerith et al., 2017; Pellis et al., 2016b) for 24, 48 and 72 h at 130 rpm. The percentage of weight loss of the enzymatic reaction was determined after the washing and drying steps of the samples.

3.5. High-Performance Liquid Chromatography (HPLC-DAD)

After the enzymatic treatment of the polyester film, the enzyme was removed via ice cold methanol precipitation. Samples were centrifuged (Hettich MIKRO 200 R, Tuttlingen, Germany) at 12,700 rpm at 0 °C for 15 min. The supernatant was filtered through 0.45 μm PTFE filters and filled into HPLC vials. For HPLC (Agilent Technologies, 1260 Infinity, Palo Alto, CA, USA) measurements, a reversed phase column C18 (Poroshell 120 EC-C18 2,7 μm 3.0 × 150 mm) was used. Analyses were carried out using H_2O/MeOH/HCOOH gradient. The flow rate was set to 0.8 mL min^{-1} with a constant temperature of 40 °C. The injection volume was 10 μL. Detection of the released products was measured with a photodiode array detector (Agilent Technologies, 1290 Infinity II, Vienna, Austria) at the wavelength of 260 nm. A 2,5-furandicarboxylic acid (for PBF) and 2,5-thiophenedicarboxylic acid (for PBTF) standard calibration curves (from 0.001 to 1 mM) were prepared and treated as described for HPLC sample preparation and used for quantification.

3.6. Scanning electron microscopy (SEM)

The surface of neat and partially hydrolyzed films was carried out on gold sputtered specimens using FE-SEM (SUPRA™ 35, Carl Zeiss SMT).

3.7. Matrix assisted laser desorption ionization (MALDI)

MALDI-TOF MS analyses on PBF and PBTF before and after enzymatic hydrolysis were carried out by using a Bruker Solarix-XR FTICR mass spectrometer and the relative software package for acquisition and processing of the data. An acceleration voltage of 25 kV, using DCTB as matrix and KTFA as ionization agent were used. 10 μL of sample were mixed with 10 μL of matrix solution (40 mg mL^{-1} DCTB in HFIP) and 3 μL of KTFA (5 mg mL^{-1}). 0.3 μL of the mixture were applied on the plate and the measurement was conducted in positive mode with the detector set in reflector mode.

4. Conclusions

The enzymatic hydrolysis of PBTF by cutinases has been for the first time demonstrated and compared to that of PBF. In 72 h of incubation, weight losses of about 20% have been reached, with PBF that seems to degrade slightly faster than PBTF. The two tested enzymes (HiC and Cut) have demonstrated better activity at higher temperatures (65 °C vs 50 °C) and HiC has shown faster kinetic of hydrolysis with respect to Cut.

Furthermore, notwithstanding the similar chemical structure, PBF and PBTF are depolymerized according to two different mechanisms: a prevalence of *exo*-wise scission has been observed for PBF, while a preferential *endo*-wise attack has been detected for PBTF. These results are correlated to the presence of the stronger interchain interactions among PBF chains, which hamper the enzyme ability to randomly cleave the ester bonds along the polymer backbone. In conclusion, the ultimate role of the chemical structure of the two five-membered heterocycles in determining not only the thermal, mechanical and barrier properties of PBF and PBTF, but also the opposite enzymatic degradation mechanism has been proven.

Abbreviations

(BSA) Bovine Serum Albumin
(PBTF) poly(1,4-butylene 2,5-thiophenedicarboxylate)
(PBF) poly(1,4-butylene 2,5-furandicarboxylate)
(Cut) *Humicola insolens* cutinase (HiC) or *Thermobifida cellulosilytic*a cutinase 1
(FDCA) 2,5-furandicarboxylic acid
(TFDCA) 2,5-thiophenedicarboxylic acid

Author contributions

The manuscript was written through contributions of all authors. All authors have given approval to the final version of the manuscript. Dr. Matteo Gigli and Mr. Felice Quartinello equally contributed to the work.

Funding sources

Dr. Alessandro Pellis thanks the FWF Erwin Schrödinger Fellowship (grant agreement: J4014-N34) for financial support. The authors from University of Bologna and University of Roma Tor Vergata acknowledge the Italian Ministry of University and Research. Mr. Felice Quartinello and Prof. Georg M. Guebitz thank the European Union's Horizon 2020 research and innovation programme (grant agreement 641942, Resyntex project) for financial support.

Declaration of Competing Interest

There are no conflicts of interest to declare.

References

Araujo, C.F., Nolasco, M.M., Ribeiro-Claro, P.J.A., Rudić, S., Silvestre, A.J.D., Vaz, P.D., Sousa, A.F., 2018. Inside PEF: chain conformation and dynamics in crystalline and amorphous domains. Macromolecules 51, 3515–3526. https://doi.org/10.1021/acs.macromol.8b00192.

de Jong, E., Dam, M.A., Sipos, L., Gruter, G.-J.M., 2012. Furandicarboxylic acid (FDCA), A versatile building block for a very interesting class of polyesters. In: Biobased Monomers, Polymers, and Materials, pp. 1–13. https://doi.org/10.1021/bk-2012-1105.ch001. Chapter 1.

Eberl, A., Heumann, S., Brückner, T., Araujo, R., Cavaco-Paulo, A., Kaufmann, F., Kroutil, W., Guebitz, G.M., 2009. Enzymatic surface hydrolysis of poly(ethylene terephthalate) and bis(benzoyloxyethyl) terephthalate by lipase and cutinase in the presence of surface active molecules. J. Biotechnol. 143, 207–212. https://doi.org/10.1016/j.jbiotec.2009.07.008.

Foekema, E.M., De Gruijter, C., Mergia, M.T., Andries van Franeker, J., Murk, A.J., Koelmans, A.A., 2013. Plastic in North Sea Fish. Environ. Sci. Technol. 47, 8818–8824. https://doi.org/10.1021/es400931b.

Gamerith, C., Vastano, M., Ghorbanpour, S.M., Zitzenbacher, S., Ribitsch, D., Zumstein, M.T., Sander, M., Herrero Acero, E., Pellis, A., Guebitz, G.M., 2017. Enzymatic degradation of aromatic and aliphatic polyesters by P. pastoris expressed cutinase 1 from Thermobifida cellulosilytica. Front. Microbiol. 8, 938. https://doi.org/10.3389/fmicb.2017.00938.

Guidotti, G., Gigli, M., Soccio, M., Lotti, N., Salatelli, E., Gazzano, M., Siracusa, V., Munari, A., 2018a. Tailoring poly(butylene 2,5-thiophenedicarboxylate) features by the introduction of adipic acid co-units: biobased and biodegradable aliphatic/aromatic polyesters. Polymer 145, 11–20. https://doi.org/10.1016/j.polymer.2018.04.063.

Guidotti, G., Soccio, M., Lotti, N., Gazzano, M., Siracusa, V., Munari, A., 2018b. Poly (propylene 2,5-thiophenedicarboxylate) vs. poly(propylene 2,5-furandicarboxylate): two examples of high gas barrier bio-based polyesters. Polymers 10, 785. https://doi.org/10.3390/polym10070785.

Guidotti, G., Gigli, M., Soccio, M., Lotti, N., Gazzano, M., Siracusa, V., Munari, A., 2018c. Ordered structures of poly(butylene 2,5-thiophenedicarboxylate) and their impact on

material functional properties. Eur. Polym. J. 106, 284–290. https://doi.org/10.1016/j.eurpolymj.2018.07.027.

Guidotti, G., Gigli, M., Soccio, M., Lotti, N., Gazzano, M., Siracusa, V., Munari, A., 2018d. Poly(butylene 2,5-thiophenedicarboxylate): an added value to the class of high gas barrier biopolyesters. Polymers 10, 167. https://doi.org/10.3390/polym10020167.

https://ec.europa.eu/commission/news/single-use-plastics-2018-may-28_en.

https://www.coca-cola.co.uk/faq/what-is-plantbottle.

Kim, M., Su, Y., Fukuoka, A., Hensen, E.J.M., Nakajima, K., 2018. Aerobic oxidation of 5-(hydroxymethyl)furfural cyclic acetal enables selective furan-2,5-dicarboxylic acid formation with CeO2-supported gold catalyst. Angew. Chem. 57, 8235–8239. https://doi.org/10.1002/anie.201805457.

Lebreton, L., Slat, B., Ferrari, F., Sainte-Rose, B., Aitken, J., Marthouse, R., Hajbane, S., Cunsolo, S., Schwarz, A., Levivier, A., Noble, K., Debeljak, P., Maral, H., Schoeneich-Argent, R., Brambini, R., Reisser, J., 2018. Evidence that the Great Pacific Garbage Patch is rapidly accumulating plastic. Sci. Rep. 8, 4666. https://doi.org/10.1038/s41598-018-22939-w.

Papageorgiou, G.Z., Tsanaktsis, V., Papageorgiou, D.G., Exarhopoulos, S., Papageorgiou, M., Bikiaris, D.N., 2014. Evaluation of polyesters from renewable resources as alternatives to the current fossil-based polymers. Phase transitions of poly(butylene 2,5-furan-dicarboxylate). Polymer 55https://doi.org/10.1016/j.polymer.2014.06.025. (38246–3858).

Papageorgiou, G.Z., Papageorgiou, D.G., Terzopoulou, Z., Bikiaris, D.N., 2016. Production of bio-based 2,5-furan dicarboxylate polyesters: recent progress and critical aspects in their synthesis and thermal properties. Eur. Polym. J. 83, 202–229. https://doi.org/10.1016/j.eurpolymj.2016.08.004.

Pellis, A., Herrero Acero, E., Weber, H., Obersriebnig, M., Breinbauer, R., Srebotnik, E., Guebitz, G.M., 2015. Biocatalyzed approach for the surface functionalization of poly (L-lactic acid) films using hydrolytic enzymes. Biotechnol. J. 10, 1739–1749. https://doi.org/10.1002/biot.201500074.

Pellis, A., Herrero Acero, E., Gardossi, L., Ferrario, V., Guebitz, G.M., 2016a. Renewable building blocks for sustainable polyesters: new biotechnological routes for greener plastics. Polym. Int. 65, 861–871. https://doi.org/10.1002/pi.5087.

Pellis, A., Haernvall, K., Pichler, C.M., Ghazaryan, G., Breinbauer, R., Guebitz, G.M., 2016b. Enzymatic hydrolysis of poly(ethylene furanoate). J. Biotechnol. 235, 47–53. https://doi.org/10.1016/j.jbiotec.2016.02.006.

Pellis, A., Comerford, J.W., Weinberger, S., Clark, J.H., Guebitz, G.M., Farmer, T.J., 2019. Enzymatic synthesis of lignin derivable pyridine based polyesters for the substitution of petroleum derived plastics. Nat. Commun. 10, 1762. https://doi.org/10.1038/s41467-019-09817-3.

Pérocheau Arnaud, S., Wu, L., Wong Chang, M.-A., Comerford, J.W., Farmer, T.J., Schmid, M., Chang, F., Li, Z., Mascal, M., 2017. New bio-based monomers: tuneable polyester properties using branched diols from biomass. Faraday Discuss. 202, 61–77. https://doi.org/10.1039/C7FD00057J.

Soccio, M., Costa, M., Lotti, N., Gazzano, M., Siracusa, V., Salatelli, E., Manaresi, P., Munari, A., 2016. Novel fully biobased poly(butylene 2,5-furanoate/diglycolate) copolymers containing ether linkages: structure-property relationships. Eur. Polym. J. 81, 397–412. https://doi.org/10.1016/j.eurpolymj.2016.06.022.

Terzopoulou, T., Karakatsianopoulou, E., Kasmi, K., Majdoub, M., Papageorgiou, G.Z., Bikiaris, D.N., 2017. Effect of catalyst type on recyclability and decomposition mechanism of poly(ethylene furanoate) biobased polyester. J. Anal. Appl. Pyrolysis 126, 357–370. https://doi.org/10.1016/j.jaap.2017.05.010.

Then, J., Wei, R., Oeser, T., Gerdts, A., Schmidt, J., Barth, M., Zimmermann, W., 2016. A disulfide bridge in the calcium binding site of a polyester hydrolase increases its thermal stability and activity against polyethylene terephthalate. FEBS Open Bio 6, 425–432. https://doi.org/10.1002/2211-5463.12053.

Wang, J., Liu, X., Zhu, J., Jiang, Y., 2017. Copolyesters based on 2,5-furandicarboxylic acid (FDCA): effect of 2,2,4,4-tetramethyl-1,3-cyclobutanediol units on their properties. Polymers 9, 305. https://doi.org/10.3390/polym9090305.

Wei, R., Oeser, T., Schmidt, J., Meier, R., Barth, M., Then, J., Zimmermann, W., 2016. Engineered bacterial polyester hydrolases efficiently degrade polyethylene terephthalate due to relieved product inhibition. Biotechnol. Bioeng. 113, 1658–1665. https://doi.org/10.1002/bit.25941.

Weinberger, S., Canadell, J., Quartinello, F., Yeniad, B., Arias, A., Pellis, A., Guebitz, G.M., 2017a. Enzymatic degradation of poly(ethylene 2,5-furanoate) powders and amorphous films. Catalysts 7, 318. https://doi.org/10.3390/catal7110318.

Weinberger, S., Haernvall, K., Scaini, D., Ghazaryan, G., Zumstein, M.T., Sander, M., Pellis, A., Guebitz, G.M., 2017b. Enzymatic surface hydrolysis of poly(ethylene furanoate) thin films of various crystallinities. Green Chem. 19, 5381–5384.

Xie, H., Wu, L., Li, B.-G., Dubois, P., 2019. Modification of poly(ethylene 2,5-furandicarboxylate) with biobased 1,5-pentanediol: significantly toughened copolyesters retaining high tensile strength and O2 barrier property. Biomacromolecules 20, 353–364. https://doi.org/10.1021/acs.biomac.8b01495.